RSC Advances

ROYAL SOCIETY OF CHEMISTRY

www.rsc.org/advances

Au nanoparticle decorated resin microspheres: Synthesis and application in electrochemical cytosensors for sensitive and selective detection of lung cancer A549 cells

Wenbo Lu, Hong-Yin Wang, Man Wang, Ying Wang, Lin Tao, Weiping Qian*

State Key Laboratory of Bioelectronics, School of Biological Science and Medical Engineering, Southeast University, Nanjing 210096, PR China

**Corresponding author: Tel: (+86)25-83795719; Fax: (+86)25-83795719. E-mail: wqian@seu.edu.cn (W. Qian)*

Abstract

In this article, for the first time, we report on a facile method for the synthesis and immobilization of AuNPs on m-aminophenol based resin (MAPR) microspheres via a simple reduction route. The AuNPs decorated MAPR (AuNPs/MAPR) microspheres with a lot of activity groups (amino and hydroxy groups) can not only act as suitable immobilization carriers for antibody (EGFR antibody), but also play an important role in facilitating the electron transfer. Moreover, the AuNPs/MAPR microspheres possess a high surface-enhanced Raman scattering (SERS) activity and have great potential as an SERS-active substrate. A novel electrochemical cytosensor which can sensitively differentiate lung cancer cells (A549 cells) from normal ones (AT II cells) by making use of the advantages of EGFR antibody and AuNPs/MAPR microspheres. EGFR antibody is immobilized on the outmost layer of the electrode surface to selectively recognize EGFR receptors over-expressed on lung cancer cells. The confocal microscopic images and cytotoxicity assays of AuNPs/MAPR microsphere confirm that the prepared cytosensors exhibit good biocompatibility, high sensitivity and selectivity for the detection of A549 cells. To the best of knowledge, it is the first cytosensors with the use of AuNPs/MAPR microspheres as carrier. It exhibits a broad linear range with a detection limit as low as 5 cells/mL, even in the presence of a large number of normal cells. Our study demonstrates that the proposed cytosensors have also been used to determine A549 cells successfully in diluted blood samples.

Keywords: Au nanoparticle; m-aminophenol; resin microsphere; SERS, lung cancer cells; cytosensor

1. Introduction

At the beginning of the 21st century, cancer has become one of the most likely causes of death worldwide [1-4]. The ever-increasing tendency of deaths from cancer has made it a top threat to human beings [1]. Diagnosing and treating cancer can be very complicated because it is not recognised as a extraneous body by our immune system [1,5]. Once cancer evolves into the phase of metastasis, other tissues of the body would be invaded and effected. However, the chance of being cured of cancer increases with early detection and treatment of the disease [1]. Therefore, the study on sensitive and accurate identification and detection of cancer cells plays a vital role in the early diagnosis and rapid exactitude therapy. Up to now, a number of conventional approaches have been developed for cancer cell detection, including fluorescent imaging, cytological testing, radiography, magnetic resonance imaging and so on [2]. Nevertheless, these methods require the expensive instrumentation and the multi-steps in preparation. Accordingly, developing a simple and rapid method for early detection of cancer is highly desirable [6,7]. To address these requirements, electrochemical cytosensors have attracted considerable attention because of the high sensitivity, rapidity, simple operation, and reproducibility [8-12]. Recently, the "target-binding" technology has been widely applied to develop electrochemical cytosensors with selectivity [3,12-14]. Wang' group have constructed an electrochemical cytosensor to selectively detect cancerous cells from normal ones based on the high affinity of folic acid for folate receptor [12]. Due to the highly specific recognition between antibody and antigen, Hu' group have reported an ultrasensitive electrochemical cytosensor for

determination of carcinoembryonic antigen (CEA)-positive cancer cells [3]. Takahashi' group has been developed an electrochemical cytosensor for the detection of cancer cells based on the specific recognition between epidermal growth factor (EGFR) receptors and EGFR antibody (anti-EGFR) [13]. However, all these above-mentioned methods suffer from more or less drawbacks such as the requirement of an extra immobilization agent [3,12] and the involvement of special enzymes [13].Accordingly, the development of new preparation strategy which can directly immobilize the antibody on the nanomaterials is highly desired.

Nowadays, Colloidal resin microsphere-based composites have attracted more and more attention because of some unique properties, containing rapid electron transfer, catalytic, specificity, and biocompatibility [15-17]. These functional resin microspheres can not only act as suitable immobilization carriers for biomacromolecules, but also have active effects on the transduction of biosensors [17]. More recently, the research on the application of Au nanoparticles (AuNPs) decorated resin microsphere has attracted great attention [17,18]. For example, Yang' group has designed the multifunctional AuNPs decorated resin microspheres for killing tumor cells through photothermy conversion [18]. Our group has reported functional resin microspheres loaded with Au nanoparticles are applied for detection of tumor markers in human serum [17]. However, the application of AuNPs decorated resin microspheres for selective detection of cancer cells is rarely reported. Accordingly, the development of a new facile strategy for application of AuNPs decorated resin microsphere in cancer cells detection is highly desired.

In this study, we report on a facile method for the synthesis and immobilization of AuNPs on m-aminophenol based resin (MAPR) microsphere via a simple reduction route for the first time. The AuNPs decorated MAPR (AuNPs/MAPR) microspheres with a lot of activity groups (amino and hydroxy groups) can not only act as suitable immobilization carriers for antibody (EGFR antibody), but also play an important role in facilitating the electron transfer. Moreover, the AuNPs/MAPR microspheres possess a high surface-enhanced Raman scattering (SERS) activity and have great potential as an SERS-active substrate. A novel electrochemical cytosensor which can sensitively differentiate lung cancer cells from normal ones by making use of the advantages of EGFR antibody and AuNPs/MAPR microspheres. EGFR antibody is immobilized on the outmost layer of the electrode surface to selectively recognize EGFR receptors over-expressed on lung cancer cells (A549 cells). It is found that the prepared cytosensors exhibit good biocompatibility, high sensitivity and selectivity for the detection of A549 cells. To the best of knowledge, it is the first cytosensors with the use of AuNPs/MAPR microspheres as carrier.

2. Materials and methods

2.1 Materials

6-(ferrocenyl) hexanethiol (6-Fc-HT) was purchased from Sigma-Aldrich Company. Nile blue A (NBA) was purchased from Alfa Aesar (USA). Rhodamine 6G (R6G), ferrocenecarboxylic acid (Fc-COOH), m-aminophenol, Bovine serum albumin (BSA), Ammonium hydroxide ($NH_3 \cdot H_2O$) (28 wt% in water), dopamine and

formaldehyde (37 wt%) were purchased from Aladin Ltd. (Shanghai, China). Chloroauric acid solution ($HAuCl_4 \cdot 4H_2O$) were purchased from Sinopharm Chemical Reagent Co., Ltd. (Shanghai, China). NaH_2PO_4, Na_2HPO_4, ethanol were purchased from Beijing Chemical Reagent (Beijing, China). Anti-EGFR polyclonal antibody standard grade antigens were purchased from Shanghai Sangon Biotech Co., LTD (Shanghai, China). All chemicals were used as received without further purification. The water used throughout all experiments was purified through a Millipore system. Phosphate buffer saline (PBS) was prepared by mixing stock solutions of NaH_2PO_4 and Na_2HPO_4. Human blood samples were kindly provided by the Hospital of Southeast University (Sipailou 2, Nanjing, China). The blood collection was approved by Institutional Review Board (IRB). The blood collection samples (Healthy, non-pregnant adults who weigh at least 50 kg) were done by venepuncture. The human serum was separated from the blood samples by centrifugation. Human serum samples were diluted to different concentrations with a PBS solution of pH 6.5, and each sample was analyzed for three times.

2.2 Instruments

Fourier Transform Infrared spectroscopy (FT-IR) measurements were made on a FT-IR Spectrometer TENSOR 27 (Bruker Optik GmbH, Ettlingen, Germany). Transmission electron microscopy (TEM) measurements were made on a HITACHI H-8100 EM (Hitachi, Tokyo, Japan) with an accelerating applied potential of 200 kV. The sample for TEM characterization was prepared by placing a drop of the dispersion on carbon-coated copper grid and dried at room temperature. Scanning

electron microscopy (SEM) measurements were made on a XL30 ESEM FEG scanning electron microscope at an accelerating applied potential of 20 kV. The sample for SEM characterization was prepared by placing a drop of the dispersion on a bare Si substrate and air-dried at room temperature. Electrochemical measurements were performed with a CHI 660D electrochemical analyzer (CH Instruments, Inc., Shanghai). A conventional three electrode cell was used, including a glassy carbon electrode (GCE, geometric area = 0.07 cm^2) as the working electrode, a Ag/AgCl (3 M KCl) electrode as the reference electrode, and platinum foil as the counter electrode. All potentials given in this work were referred to the Ag/AgCl electrode. All the experiments were carried out at ambient temperature.

2.3 Synthesis of MAPR microspheres

MAPR microspheres were prepared according to reported method with a little modification [19]. In a typical synthesis, 0.051g of m-aminophenol was added into 13 mL of ethanol and 5 mL of water, followed by adding 56.5 μL of ammonia aqueous solution (NH_4OH, 28 wt%) to form a homogeneous solution for 30 min at 35 ℃. After the addition of 46 μL of formaldehyde solution (37 wt%), the resulting mixed solution was stirred at 40 ℃ for 200 min and subsequently heated at 100 ℃ for 24 h in a Teflon-lined autoclave. The resin spheres were purified with distilled water and ethanol by centrifugation at a speed of 5000 rpm for 3 times, respectively. The MAPR microspheres were collected by centrifugation and washed with doubly distilled water to remove some small spheres in the mixture. The obtained precipitates (MAPR microspheres) were redispersed in 20 mL of water for characterization and further

use.

2.4 Synthesis of AuNPs decorated MAPR microspheres

In a typical synthesis, firstly, 200 μL of 24.3 mM $HAuCl_4$ solution was added into 8 mL of MAPR microspheres dispersion, and then the mixture solution was stirred for 30 min. Next, 100 μL of 0.10 M $NaBH_4$ aqueous solution were added into the previous solution under stirring for 30 min at room temperature. The precipitate was collected by centrifugation and washed with water twice. The resultant AuNP/MAPR microspheres were redispersed in 1 mL of H_2O for characterization and further use.

2.5 SERS Measurements

The AuNP/MAPR microspheres are immobilized on ITO surfaces by using electrostatically assisted APTES-functionalized surface-assembly as SERS active substrates. The ITO glass slips were washed with ultrapure water for at least three times. The slips were further cleaned in ethanol with sonication for three times and dried at 60 ^oC for 2 h in an air oven. The cleaned ITO glass slips were vertically immersed in a 1% (v/v) ethanol solution of APTES in anhydrous ethanol for 2 h, rinsed three times in ethanol with sonication to remove silane excess and dried in an air oven.

Then, the functional ITO glass slips are dipped overnight into the stirred colloidal suspension of AuNP/MAPR microspheres in order to form AuNP/MAPR layers. For subsequent SERS experiments, the NBA and R6G are used as the analytes. The AuNP/MAPR layer decorated ITO substrates previously described were first

vertically immersed in each analyte aqueous solution with a series of NBA or R6G concentrations for 6 h and then left to dry at room temperature for SERS measurements. The Raman experiments were collected with a Renishaw Invia Reflex system equipped with Peltiercooled charge-coupled device (CCD) detectors and a Leica microscope. Samples were excited with a 785 nm diode laser under line-focus mode and the laser power was adjust to 0.5%, which was about 0.06 mW. The corresponding laser was focused onto the sample surface using a 50 × long working distance objective. Spectra were collected in continuous mode with 10 s exposure time and accumulated twice and a grating of 1200 mm^{-1} was used. Every SERS spectrum was averaged from 5 measurements. All experiments were performed in triplicate and values were averaged.

2.6 Fabrication of the cytosensor

1 mL AuNPs/MAPR microspheres dispersion solution is added in 5 mL water contain 2 mM of 6-Fc-HT solution, and then the mixture solution was stirred for 2 h. AuNPs are covalently attached to the 6-Fc-HT with the thiol-terminated surface, Au-S bonding can be formed between the AuNPs/MAPR microspheres and the surface thiol-groups of 6-Fc-HT. The precipitate was collected by centrifugation in order to remove unreacted 6-Fc-HT and redispersed in 1 mL of H_2O. The GCE was firstly immersed into 1 % chitosan solution for 1 h. Then, 2 μL of 6-Fc-HT/AuNPs/MAPR microspheres was dropped on the surface of pretreated GCE and left to dry at room temperature. The 6-Fc-HT/AuNPs/MAPR microspheres modified GCE (6-Fc-HT/AuNPs/MAPR/GCE) was immersed into the mixture of 20

mM NHS and 100 mM EDC in water for 2 h at room temperature to activate the terminal carboxylate group of the microspheres and rinsed with water. After washing, anti-EGFR was immediately dropped on the surface of the modified electrode and then incubated for 100 min to form the anti-EGFR/6-Fc-HT/AuNPs/MAPR/GCE. Following that, this electrode was washed and incubated in 1 wt% BSA solution for 60 min to eliminate nonspecific binding. The cytosensor, anti-EGFR/6-Fc-HT/AuNPs/MAPR/GCE, was thus fabricated and used for the cell detection. Scheme 1 displays the measurement protocol of the electrochemical cytosensor fabrication procedure.

Scheme 1

2.7 Cell culture and detection

Human lung adenocarcinoma cell line (A549) and human type Ⅱ alveolar epithelial cell line (AT II) were obtained from Medical School of Southeast University. They were cultured in Dulbecco's modified eagle medium (DMEM) supplemented with 10% fetal bovine serum (FBS) and 1% penicillin streptomycin solution, and incubated at 37 ℃ and 5 % CO_2 environment. The cells were trypsinized and subcultured every two days. The cell number was detected using a Petroff Hausser cell counter.

For immobilization on the surface of the cytosensor, the cells were separated from the medium by centrifugation at 1500 rpm for 3 min and then washed three times with PBS. The precipitate was carefully redispersed in PBS to obtain a homogeneous cell suspension at a certain concentration. Finally, the

anti-EGFR/AuNPs/MAPR microsphere-electrode was immersed into the cell suspensions for 30 min. Square wave voltammetry (SWV) is performed for cell detection because it is very sensitive to current signal change. The SWV spectra are collected by the prepared cytosensor after being incubated in A549 cell suspensions with different concentrations.

2.8 Confocal imaging

These ITO slices coated with AuNPs/MAPR microsphere layer/anti-EGFR films were prepared and then placed in a 10 cm cell culture plate. Then A549 or AT II cells were introduced into the plate and cultured in DMEM medium supplemented with 10% FBS at 37 ^{o}C. At the time of 15, 30 and 60 h, one of the ITO slices was taken out and the cells on which were stained with Rhodamine 123. The fluorescent images of cells are quickly observed under a confocal laser-scanning microscope (CLSM, Leica TCS-SP8).

2.9 Cytotoxicity of AuNPs/MAPR microspheres

The cytotoxicity of AuNPs/MAPR microspheres to A549 cancer cells and AT II normal cells were evaluated using MTT assay. Cells were cultured in Dulbecco's modified Eagle's medium (DMEM), supplemented with 10 % fetal bovine serum (FBS) and 100 IU/mL penicillin-streptomycin at 37 ^{o}C in a humid atmosphere with 5 % CO_2. For MTT assay, cells were seeded onto 96-well plates at a density of 5×10^3 cells per well in 100 μL complete culture medium. After culturing for one day when the cells grew to 80 % confluence in each well, the medium was replaced with 100 μL fresh medium containing different concentrations of AuNPs/MAPR microspheres and

further cultured for 24 h. Then, 10 μL MTT solution (5 mg/mL in cell PBS) was added into each well directly and the cells were incubated for an additional 4 h at 37 ^{o}C. After that, the medium was carefully aspirated. The cells were solubilized in 150 μL DMSO, and then absorbance at 492 nm was measured against a background control using a microplate reader (Thermo-scientific, Multiskan FC, USA).

3. Results and discussion

Figure 1

The structure of the as-prepared MAPR microspheres was first characterized by SEM. Figure 1A shows a representative SEM images of the as-prepared product, which consists exclusively of a large amount of sub-microspheres. The magnified SEM image of these sub-microspheres demonstrates that the MAPR microspheres are about 300 to 400 nm in diameter, as shown in Figure 1B. Figure 1C shows the low magnification SEM images of AuNPs/MPAR microspheres, which consists exclusively of a large amount of sub-microspheres. A large amount of small nanoparticles are adsorbed on the surface of MAPR microspheres, as shown in Figure 1C. The high magnification SEM image shown in Figure 1D further reveals the AuNPs/MPAR microspheres have a behavior of very dense nanoparticles. The TEM image shows a large amount of AuNPs are deposited onto the surface of the exterior of MAPR microspheres in Figure S1. The MAPR microspheres have the branched chain of amino group and hydroxyl group, due to the synthesis of raw materials (m-aminophenol). The existence of amino group and hydroxyl group will be further

proved by FT-IR spectra. These functional groups of MAPR microspheres can act as suitable adsorption carriers for Au^{3+} ion. The reduction of these Au^{3+} ions by sodium borohydride allows these AuNPs to attach onto the MAPR microspheres. Meanwhile, these functional groups of MAPR microspheres can also favor the immobilization of antibody (EGFR antibody) by carboxyl-to-amine crosslinker reaction.

Figure 2

SERS spectroscopy has received a great deal of attention for its utility as a sensitive technique for biomedical analysis [20]. The metallic nanomaterials exhibit high SERS activity, due to an increased field at the metallic nanoparticle surface which is a consequence of the interaction of the incoming laser radiation with electrons in the metal surface or collective oscillations of the metal electrons [21]. To study the SERS activity of the AuNPs/MAPR microspheres, two organic molecules, NBA and R6G, are used to testify the SERS activities of the substrates. The latter molecule, R6G is often employed in SERS studies because of its large Raman cross-section. The AuNPs/MAPR microspheres, are adopted as the standard probe to enhance the Raman signals in the following experiments. Figure 2A shows the obtained SERS spectra when different concentrations (1×10^{-9} M up to 1×10^{-5} M, line a to line e in Figure 2A) of R6G solutions were tested. As shown in Figure 2A, the typical SERS spectra of R6G are characterized by the prominent strong bands at 613, 776, 1181,1315, 1364, and 1511cm^{-1}, assigned to the typical aromatic benzene ring breathing and stretching vibrational modes [22]. The SERS signals increased proportionally with the increasing concentration of R6G, which can be utilized as a

quantitative measurement of R6G concentration. As shown in Figure 2C, the calibration plots show a good linear relationship between the SERS signals and the logarithm values of the concentrations of R6G. The peak at 1511 cm^{-1} of the R6G molecule is chosen as reference peak in the study. It is obviously seen that there is a linear relationship between the SERS signals and the concentration of R6G over the range of 1×10^{-9} M up to 1×10^{-5} M with a correlation coefficient of 0.993, as shown in Figure 2C. The spectra obtained when the substrate was immersed in NBA solutions of different concentrations in Figure 2B (line a to line e), following the same procedure from low to high concentration as that in the R6G measurements. The peak at 592 cm^{-1} of the NBA molecule is chosen as reference peak in the study. It is obviously seen that there is a linear relationship between the SERS signals and the concentration of NBA over the range of 1×10^{-7} M up to 5×10^{-5} M with a correlation coefficient of 0.995, as shown in Figure 2D. All above observations indicate the as-prepared AuNPs/MAPR microspheres exhibit high SERS activity.

Figure 3

To investigate whether AuNPs/MARP microspheres is suitable for practical applications, and the cytotoxicity of AuNPs/MARP microspheres is evaluated against A549 cells (Figure 3A) and AT II cells (Figure 3B). The effect of AuNPs/MARP microspheres on A549 cell and AT II cell survival is investigated by MTT assay. As shown in Figure 3, A549 cells and AT II cells are treated with different concentrations (0, 0.4, 0.8, 1.6, 3.2, 6.4, 12.8 and 25.6 mg/mL) of AuNPs/MARP microsphere dispersions for 24 h and then the viability is tested. Some of concentrations of

AuNP/MARP microspheres result in viability values of more than 100% (100% is the viability of the control), indicating that AuNP/MARP microspheres show no toxicity at a certain concentration and promote cell proliferation. As a result, MTT assay results shown in Figure 3 reveals that no cytotoxicity is observed after 24 h incubation.

Figure 4

Figure 4A shows FT-IR results for the MAPR microspheres. The peak at 1225 cm^{-1} is assigned to the C-OH stretching [25]. The peak observed at 1624 cm^{-1} can be attributed to a stretching of the secondary amine of the m-aminophenol in MAPR microspheres [26]. The peak of the -N-H absorption bands are also observed at 3367 cm^{-1} [27], as shown in Figure 4A. The -OH of the carboxylic group stretching peak is also observed at 3740 cm^{-1} [28]. It is observed that the bonds of the -OH groups, the carboxylic (-COOH) group and amines (-NH) are presented in the MAPR microspheres, suggesting that AuNPs can easily adsorb on the exterior of MAPR microspheres. Figure 4B shows FT-IR results for the AuNPs/MAPR microspheres. These characteristic absorption bands observed at 1624 cm^{-1}, 3367 cm^{-1} and 3740 cm^{-1} are also observed in the FT-IR spectrum of the AuNPs/MAPR microspheres [26-28]. It is observed that the bonds of the -OH groups and the carboxylic (-COOH) group are presented in the AuNPs/MAPR microspheres, which can provide a favorable microenvironment for immobilization of anti-EGFR without additional immobilized reagent. The FT-IR spectrum of 6-Fc-HT/AuNPs/MAPR microspheres show several peaks in Figure 4C. A series of characteristic vibrational modes centered

around 887, 1002, 1710 cm^{-1} are the characteristic absorption peak of ferrocene is assigned as the D5d symmetry [29], revealing that the 6-Fc-HT/AuNPs/MAPR microspheres are successfully prepared. Figure 4D shows the FT-IR spectrum of anti-EGFR/6-Fc-HT/AuNPs/MAPR microspheres. The peak at 1649 cm^{-1} is assigned to the C=O symmetric stretching band of C=O group [30]. The peaks of the characteristic absorption bands of ferrocene are also observed at 1002 and 1105 cm^{-1}, as shown in Figure 3D. The peak at 1551 cm^{-1} is characteristic asymmetric stretching modes in –CONH- of antibody [30], indicating that the anti-EGFR are successfully decorated the 6-Fc-HT/AuNPs/MAPR microspheres.

Figure 5

Electrochemical impedance spectroscopy (EIS) is an effective tool for monitoring the interfacial properties of electrode during the modification process [31]. In the Nyquist diagram, the linear portion at the low frequencies and the semicircle portion at the high frequencies correspond to the diffusion-limited process and the electron transfer-limited process, respectively. The electron transfer resistance can be estimated from the diameter of a semicircle in an impedance spectrum. Figure 5A shows the complex impedance plots of different layer modified electrode in 5.0 mM $[Fe(CN)_6]^{4-/3-}$ solution. It is observed that the bare GCE exhibits a small semicircle at high frequencies with a diameter of 143 ohm and a linear part at low frequencies (line a of Figure 5A), which is characteristic of a diffusional limiting step of the electrochemical process on a bare GCE. After deposition of 6-Fc-HT/AuNPs/MAPR microspheres (line b of Figure 5A), the Ret of 97 ohm is much smaller than that of the

bare GCE, indicating that the 6-Fc-HT/AuNPs/MAPR composites can promote the electron transfer. While the anti-EGFR is adsorbed to the 6-Fc-HT/AuNPs/MAPR/GCE (line c of Figure 5A), the value of Ret increased to 182 ohm. The result is ascribed to the nonconductive properties of anti-EGFR which insulates the conductive support and blocks the electron transfer. Similarly, after the capture of BSA and A549 cells, the values of Ret increase to 219 ohm and 311 ohm, as shown in line d and line e of Figure 5A, respectively. It is suggested that the formation of nonconductive and hydrophobic immunocomplex layer hinders the electron transfer. All these observations demonstrate that the 6-Fc-HT/AuNPs/MAPR microspheres, anti-EGFR, BSA and A549 cells have been successively assembled on to the GCE.

Figure 5B shows current responses of the anti-EGFR/6-Fc-HT/AuNPs/MAPR/GCE in supporting electrolyte. It is observed that a pair of redox peaks with high magnitude are shown in the line a of Figure 5B. The apparent formal potential was calculated as 0.35 V from the average of oxidation and reduction peak potentials. As a control experiment is carried out, the Fc-COOH decorated MAPR microspheres modified the GCE, producing a anti-EGFR/Fc-COOH/MAPR/GCE. However, the current response of the anti-EGFR/Fc-COOH/MAPR/GCE (line b of Figure 5B) is lower than that of the anti-EGFR/6-Fc-HT/AuNPs/MAPR/GCE (line a of Figure 5B). This can be attributed to the magnification function of the assembled AuNPs coated on the MAPR microspheres, beacuse the AuNPs can facilitate electron transfer between surface

immobilized protein and the underlying electrode [32]. The relationship between scan rate and peak current is very important in understanding the electrochemical mechanism. The cyclic voltammograms (CVs) of the proposed cytosensor (the anti-EGFR/6-Fc-HT/AuNPs/MAPR/GCE) in 5.0 mM $[Fe(CN)_6]^{4-/3-}$ solution at different scan rates are investigated in the range of 20–200 mV s^{-1}. It is clearly seen that the potentials and peak currents are dependent on the scan rate in Figure 5C. The peak current is enhanced when the scan rate increased. As shown in Figure 5D, linear relationships with good correlation coefficients are observed between the peak current and the scan rate in the range between 10 and 200 mV s^{-1}, suggesting that the redox process of the ferrocene of the 6-Fc-HT/AuNPs/MAPR microspheres on the electrode surface is a fast and surface-confined process.

Figure 6

The evaluation of A549 and AT II cells with electrochemical methods is also investigated by the fibered confocal fluorescence microscopy. The A549 cells are adhered to the cytosensor surface. The viability of cells on the cytosensor is easily affected by the physical and chemical properties of the cytosensor. The biocompatible property of the cytosensor is investigated by monitoring A549 cells proliferation on anti-EGFR/6-Fc-HT/AuNPs/MAPR decorated ITO surface, as shown in Figure 6 (A-C). The density of cultured A549 cells on the anti-EGFR/6-Fc-HT/AuNPs/MAPR decorated ITO surface increases with the extended incubation time, confirming that A549 cells can grow and proliferate very well on the anti-EGFR/6-Fc-HT/AuNPs/MAPR decorated ITO surface. It is obviously seen that

the proliferated A549 cells have a good viability after incubation for 60 h, due to the morphology of the distinguishable filopodia [14], as shown in Figure 6C. We also performed one control experiment by monitoring AT II cells proliferation on anti-EGFR/6-Fc-HT/AuNPs/MAPR decorated ITO surface, as shown in Figure 6D and Figure 6E. As is known to all, cancer cells divide more rapidly than normal cells. As a result, AT II cells (Figure 6E) proliferation is slower than A549 cells (Figure 6C) after incubation for 60 h. The proliferated AT II cells with a good viability is shown in Figure 6E. All the above observations indicate that our prepared cytosensor exhibits excellent biocompatible property.

The specificity of anti-EGFR which possibly can be cross-reacted with normal cells is investigated by carrying out the two control experiments. As shown in Figure 6F (line b), when the anti-EGFR is decorated the cytosensor, the peak current (△I) of A549 cells is obvious, while the peak current (△I) of AT II cells is quite small. When the anti-EGFR is absent, both of the corresponding response are quite weak in Figure 6F (line a). These observations indicate that the cross-reactivity could be ignored.

Figure 7

Figure 7A shows the square wave voltammetry (SWV) responses of the cytosensor after being incubated in the different concentrations of A549 cells suspensions. A549 cells are attached to the electrode surface through immunoreaction with anti-EGFR which was immobilized on the cytosensor previously. The insulating A549 cells layer acting as a nonconductor obstructed the electron transfer between the electrolyte and electrode surface. Therefore, the SWV peak currents decreased

proportionally with the increasing concentration of A549 cells, which can be utilized as a quantitative measurement of A549 cells concentration. Figure 7A shows that the peak current decreases with the increasing concentration of A549 cells. As shown in Figure 7B, the calibration plots show a good linear relationship between the peak currents and the logarithm values of the A549 cell concentrations. It is obviously seen that there is a linear relationship between the peak currents and the concentration of A549 cells over the range of 5–10^6 cells/mL with a correlation coefficient of 0.994, suggesting a wide detection range and a detection limit as low as 5 cells/mL. Table S1 (Supporting information) compares the sensing performance of different cytosensors for detection of cancer cells, showing our proposed cytosensor exhibits a lower detection limit than the results of previously reported sensing systems.

The selectivity of the prepared cytosensor is further evaluated in this study. SWV is also applied to monitor A549 cells in the presence of normal cells [human type II alveolar epithelial cell line (AT II cells)]. It is well-known that the EGFR receptors can be acted as the tumor indicator. The EGFR receptors are overexpressed on the lung cancer cells (A549 cells) while limitedly expressed on the normal lung cells [13]. As a result, the proposed cytosensor can selectively detect A549 cells in the presence of AT II cells, due to the special recognition between anti-EGFR and EGFR receptors. Figure 7C shows the SWV responses of the cytosensor after being incubated in the different concentrations of A549 cells suspensions in the presence of AT II cells. It is obviously seen that the SWV peak current intensity proportionally decreased with the A549 cell concentrations in Figure 7C. The calibration plots show a good linear

relationship between the peak currents and the logarithm values of the A549 cell concentration in the range from 0 to 10^6 A549 cells/mL with a correlation coefficient of 0.993, as shown in Figure 7D. A detection limit as low as 5 cells/mL is obtained in the presence of a large number of AT II cells (10^4 cells/mL), indicating that the prepared cytosensors exhibit the high selectivity as well as high sensitivity. The detection limit is better than the previously reported cytosensors [9,10,12]. All these observations confirm that the cytosensors show a wider detection range and the detection can be finished quickly within half a minute, avoiding possible contamination on the cells.

Direct determination of cancer cells level in blood serum plays an important role in the early detection of cancer. To testify the feasibility of the cytosensor in practical analysis, we employed the cytosensor to measure A549 cells concentration in human serum samples. The electrolyte solution containing 5 mL of the serum sample is used for SW voltammetry experiment. The calibration plots showed a linear relationship between the peak currents and the logarithm values of the A549 cell concentrations in Figure S2 (Supporting information). It is obviously seen that there is a linear relationship between the peak currents and the concentration of A549 cells over the range of 0--10^6 cells/mL with a correlation coefficient of 0.98, as shown in Figure S2. A detection limit as low as 10 cells/mL is obtained in human serum samples. All the above observations indicate that the biosensor offers a method to detect A549 cell concentration in human serum samples.

4. Conclusions

In summary, a facile method for the synthesis and immobilization of small AuNPs on MAPR microsphere via a simple reduction route is reported for the first time. The AuNPs/MAPR microspheres not only possess a high surface enhanced Raman scattering (SERS) activity and have great potential as an SERS-active substrate, but also play an important role in facilitating the electron transfer. A novel electrochemical cytosensor which can sensitively differentiate lung cancer cells from normal ones by making use of the advantages of EGFR antibody and AuNPs/MAPR microspheres. The prepared cytosensors exhibit good biocompatibility, high sensitivity and selectivity for the detection of A549 cells, which exhibit great potential for application in the development of biosensors.

Acknowledgements

We gratefully acknowledge supports from the Chinese 973 Project (Grant: 2012CB933302), the National Natural Science Foundation of China (Grant: 21175022), the Ministry of Science & Technology of China (Grant: 2012AA022703), the Scientific Research Foundation of Graduate School of Southeast University (No.YBJJ1410), the Fundamental Research Funds for the Central Universities (No. 2242014Y10054) and Graduate Students' Scientific Research Innovation Project of Jiangsu Province Ordinary University (No.CXZZ13_0124).

References

[1] G. Zhang, X. Zeng, P. Li, *J. Biomed. Nanotechnol.* 2013, **9**, 741.

[2] M. Perfezou, A. Turner, A. Merkoci, *Chem. Soc. Rev.* 2012, **41**, 2606.

[3] C. Hu, D. Yang, Z. Wang, L. Yu, J. Zhang, N. Jia, *Anal. Chem.* 2013, **85**, 5200.

[4] Y. Wang, Z. Li, D. Hu, C. Lin, J. Li, Y. Lin, *J. Am. Chem. Soc.* 2010, **132**, 9274.

[5] G. Nie, Z. Bai, W. Yu, J. Chen, *Biomacromolecules*, 2013, **14**, 834.

[6] Y. Qin, J. Liu, D. Li, L. Xu, Y. Liu, E. Wang, *Electrochem. Commun.* 2012, **18**, 81.

[7] T. Kwon, J. Park, G. Lee, K. Nam, Y. Huh, S. Lee, J. Yang, C. Lee, K. Eom, *J. Phys. Chem. Lett.* 2013, **4**, 1126.

[8] X. Wang, J. Ju, J. Li, J. Li, Q. Qian, C. Mao, J. Shen, *Electrochim. Acta*, 2014, **123**, 511.

[9] S. Xu, J. Liu, T. Wang, H. Li, Y. Miao, Y. Liu, J. Wang, E. Wang, *Talanta* 2013, **104**, 122.

[10] R. Wang, J. Di, J. Ma, Z. Ma, *Electrochim. Acta* 2012, **61**, 179.

[11] T. Zheng, Q. Zhang, S. Feng, J. Zhu, Q. Wang, H. Wang, *J. Am. Chem. Soc.* 2014, **136**, 2288.

[12] H. Li, D. Li, J. Liu, Y. Qin, J. Ren, S. Xu, Y. Liu, D. Mayer, E. Wang, *Chem. Commun.* 2012, **48**, 2594.

[13] Y. Takahashi, T. Miyamoto, H. Shiku, R. Asano, T. Yasukawa, I. Kumagai, T. Matsue, *Anal. Chem.* 2009, **81**, 2785.

[14] J. Liu, Y. Qin, D. Li, T. Wang, Y. Liu, J. Wang, E. Wang, *Biosens. Bioelectron.*

2013, **41**, 436.

[15] K. Mori, M. Dojo, H. Yamashita, *ACS Catalysis* 2013, **3**, 1114.

[16] Y. Wu, Y. Li, L. Qin, F. Yang, D. Wu, *J. Mater. Chem. B* **2013,** 1, 204.

[17] W. Lu, C. Qian, L. Bi, L. Tao, J. Ge, J. Dong, W. Qian, *Biosens. Bioelectron.* 2014, **53**, 346.

[18] P. Yang, Q. Xu, S. Jin, Y. Zhao, Y. Lu, X. Xu, S. Yu, *Chem. Eur. J.* 2012, **18**, 1154.

[19] J. Zhao, W. Niu, L. Zhang, H. Cai, M. Han, Y. Yuan, S. Majeed, S. Anjum, G. Xu, *Macromolecules* 2013, **46**, 140.

[20] S. Bell, N. Sirimuthu, *J. Am. Chem. Soc.* 2006, **128**, 15580.

[21] E. Esenturk, A. Walker, *J. Raman Spectrosc.* 2009, **40**, 86.

[22] T. Quyen, C. Chang, W. Su, Y. Uen, C. Pan, J. Liu, J. Rick, K. Lin, B. Hwang, *J. Mater. Chem. B*, 2014, **2**, 629.

[23] E.C. LeRu, E. Blacjie, M. Meyer, P.G. Etchegoin, *J. Phys. Chem. C* 2007, **111**, 13794.

[24] Q. Su, X. Ma, J. Dong, C. Jiang, W. Qian, *ACS Appl. Mater. Interfaces* 2011, **3**, 1873.

[25] W. Sun, S. Shi, T. Yao, *Anal. Mehtods* 2011, **3**, 2472.

[26] N.R. Sheela, S. Muthu, S.S. Krishnan, *Asian J. Chem.* 2010, **22**, 5049.

[27] B. Tran, M.P. Washington, D.A. Henckel, X. Gao, H. Park, M. Pink, D.J. Mindiola, *Chem. Commun.* 2012, **48**, 1529.

[28] Y. Inokuchi, K. Ohashi, Y. Honkawa, N. Yamamoto, H. Sekiya, N. Nishi, *J. Phys.*

Chem. A 2003, **107**, 4230.

[29] H. Qiu, Z. Wang, Z. Shi, Z. Gu, J. Qiu, *Acta Phys. Chim. Sin.* 2007, **23**, 1451.

[30] M. Li, S.K. Cushing, J. Zhang, S. Suri, R. Evans, W.P. Petros, L.F. Gibson, D. Ma, Y. Liu, N. Wu, *ACS Nano* 2013, **7**, 4967.

[31] E. Katz, I. Willner, *Electroanalysis* 2003, **15**, 913.

[32] J.M. Pingarron, P. Yanez-Sedeno,A.Gonzalez-Cortes, *Electrochim. Acta* 2008, **53**, 5848.

Figure captions:

Scheme 1 Schematic illustration of the stepwise electrochemical cytosensor fabrication process.

Figure 1 (A) Low and (B) high magnification SEM images of the MAPR microspheres. (C) Low and (D) high magnification SEM images of the AuNPs/MAPR microspheres.

Figure 2 (A) Representative 785 nm excited SERS spectra with different concentrations of R6G : (a) 10^{-5} M, (b) 10^{-6} M, (c) 10^{-7} M, (d) 10^{-8} M, (e) 10^{-9} M on AuNPs/MAPR microspheres. (C) A logarithmic plot of R6G concentration and the intensity of SERS signal for the bands at 1511 cm^{-1}. (B) Representative 785 nm excited SERS spectra with different concentrations of NBA : (a) 5×10^{-5} M, (b) 5×10^{-6} M, (c) 1×10^{-6} M, (d) 5×10^{-7} M, (e) 1×10^{-7} M on AuNPs/MAPR microspheres. (D) A logarithmic plot of NBA concentration and the intensity of SERS signal for the bands at 592 cm^{-1}.

Figure 3 Cytotoxicity of the tested AuNPs/MARP microspheres against the A549 cells (A) and the AT II cells (B).

Figure 4 FT-IR spectra of MAPR microsphere (A), AuNPs/MAPR microspheres (B), 6-Fc-HT/AuNPs/MAPR microspheres (C) and anti-EGFR/6-Fc-HT/AuNPs/MAPR microspheres (D).

Figure 5 (A) Nyquist plots of the EIS for each immobilized step recorded from 0.1 to 10^5 Hz of bare GCE (a), 6-Fc-HT/AuNPs/MAPR/GCE (b), anti-EGFR/6-Fc-HT/AuNPs/MAPR/GCE (c), BSA/anti-EGFR/6-Fc-HT/AuNPs/MAPR/GCE (d), and A549 cells/BSA/anti-EGFR/6-Fc-HT/AuNPs/MAPR/GCE (e) in 1 mM $[Fe(CN)_6]^{3-/4-}$ solution. (B) Cyclic voltammograms (CVs) of the anti-EGFR/6-Fc-HT/AuNPs/MAPR/GCE (a) and the anti-EGFR/Fc-COOH/MAPR/GCE (b) in supporting electrolyte at a scan rate of 100 mV/s. (C) CVs of the modified electrodes at different scan rates (from inner to outer): 10, 20, 50, 80, 100, 150, 200 mV/s. (D) The calibration plots between the dependence

of redox peak currents and the potential scan rates.

Figure 6 Fibered confocal fluorescence microscopy images of A549 cells on the anti-EGFR/6-Fc-HT/AuNPs/MAPR decorated ITO surface for 15 h (A), 30 h (B) and 60 h (C). The images of AT II cells on the modified ITO surface for 30 h (D) and 60 h (E). (F) SWV responses of the AuNPs/MAPR/GCE (a) and anti-EGFR/AuNPs/MAPR/GCE (b) after incubation in 1×10^{-3} cells/mL of A549 cell solution and 1×10^{-3} cells/mL of AT II cell solution, respectively.

Figure 7 (A) SWV responses of the anti-EGFR/6-Fc-HT/AuNPs/MAPR/GCE after being incubated with different concentrations of A549 cells in 0.1 M PBS (pH: 7.4) solution : 0, 5, 10, 10^2, 10^3, 10^4, 10^5, 10^6 cells/mL (from bottom to top). (B) The calibration plots of the changes of the SWV current responses via the logarithm values of A549 cell concentrations. (C) SWV responses of the anti-EGFR/6-Fc-HT/AuNPs/MAPR/GCE after being incubated with different concentrations of A549 cells in the presence of 10^4 cells/mL AT II cells (from bottom to top: 0, 5, 10, 10^2, 10^3, 10^4, 10^5, 10^6 cells/mL A549 cells). (D) The calibration plots of the changes of the SWV peak current intensity via the logarithm values of A549 cell concentrations in 0.1 M PBS (pH: 7.4) solution.

Figures:

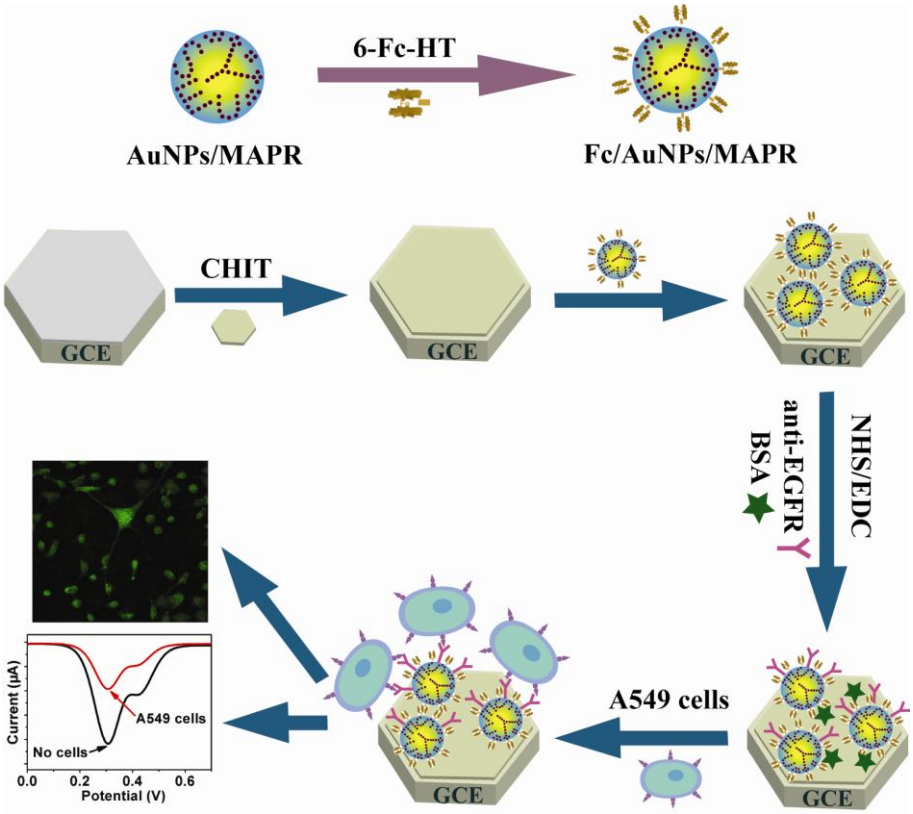

Scheme 1

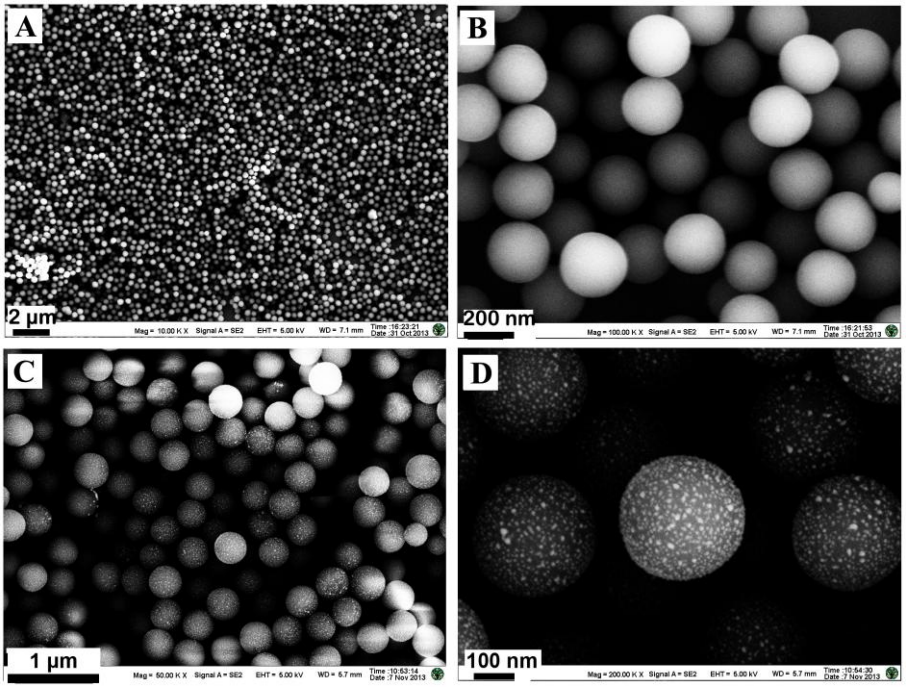

Figure 1

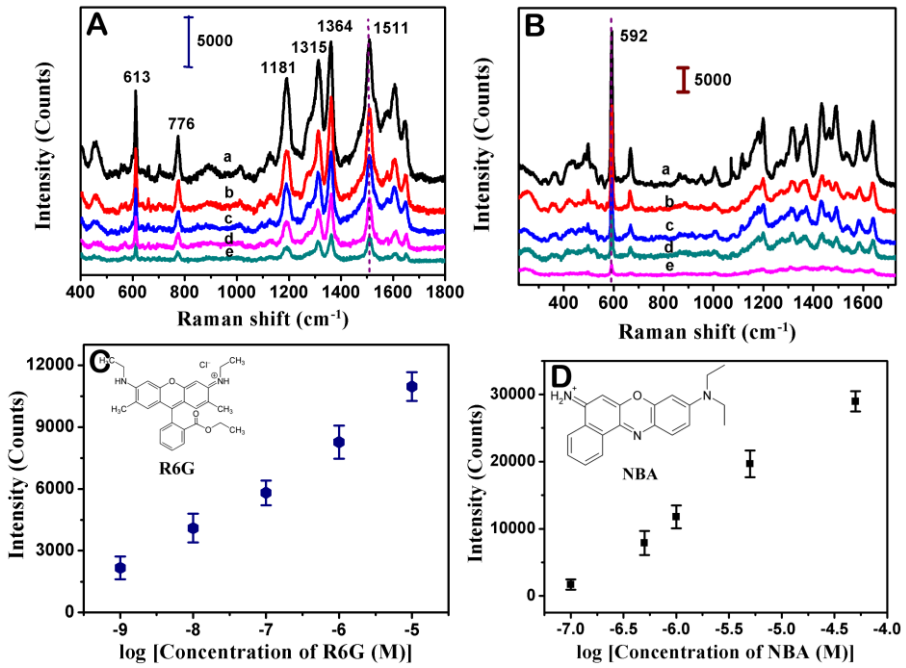

Figure 2

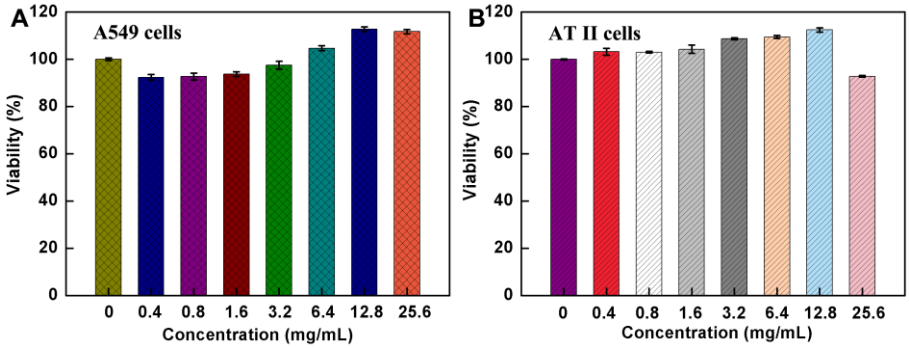

Figure 3

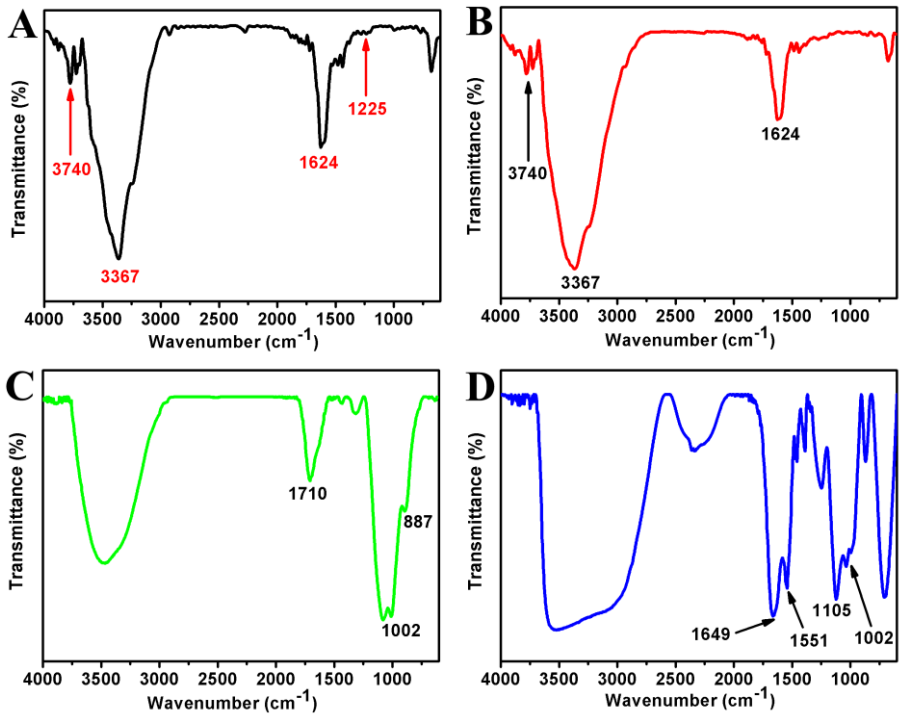

Figure 4

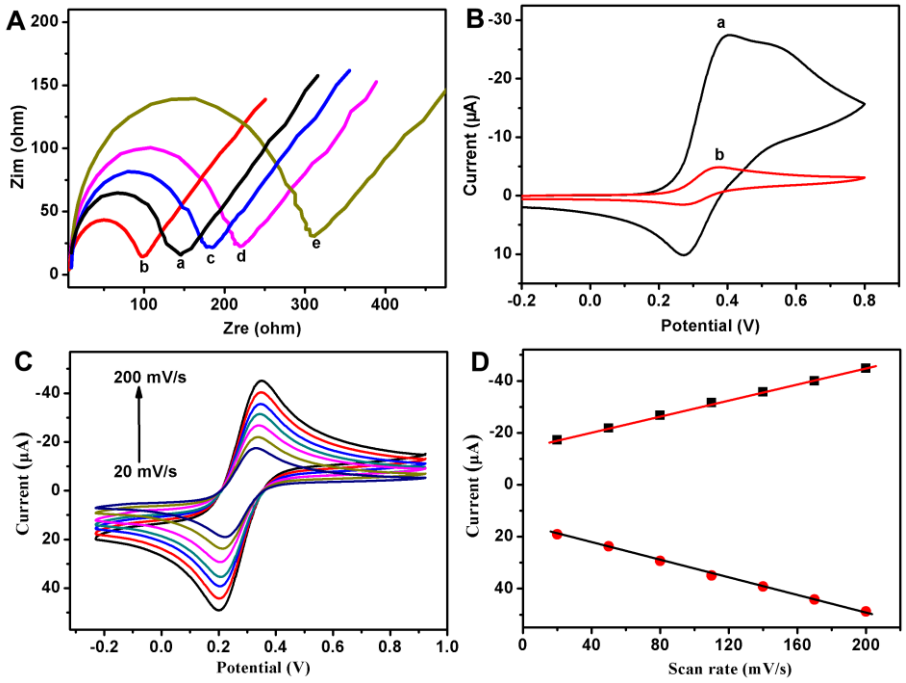

Figure 5

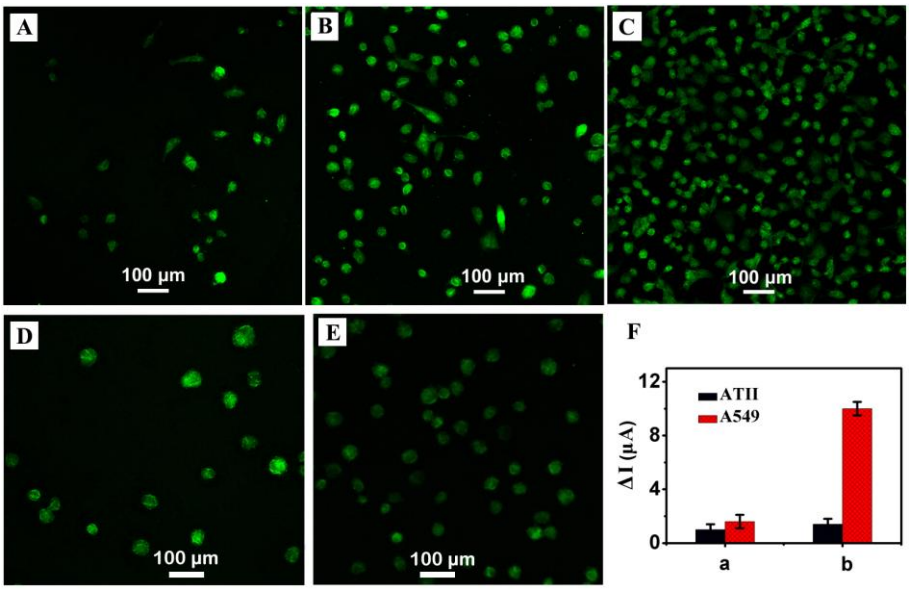

Figure 6

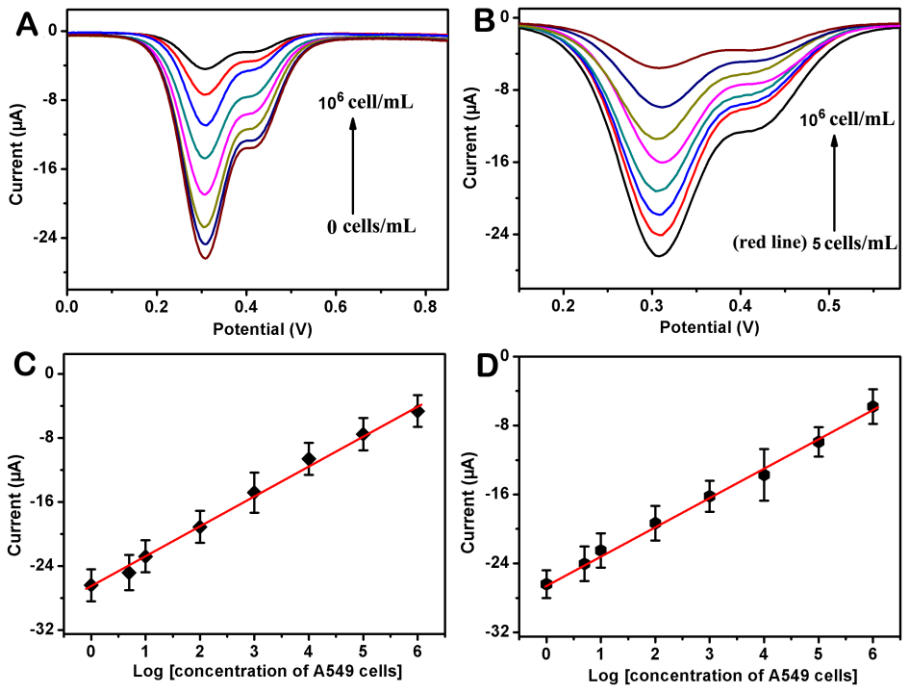

Figure 7